

Effect of Complex Alloying on the Phase Composition and Thermal Characteristics of Al–Fe–Si Aluminum Alloys

Andreyachshenko V.A.

Abylkas Saginov Karaganda Technical University, Karaganda, Kazakhstan

Corresponding author email: v.andreyachshenko@ktu.edu.kz

<p>Received: September 8, 2025 Peer-reviewed: September 26, 2025 Accepted: October 3, 2025</p>	<p>ABSTRACT This study presents a comprehensive analysis of phase formation in Al–Fe–Si aluminum alloys with the addition of ten industrially significant alloying elements (Mg, Cu, Ni, Mn, Cr, Zn, Ti, Zr, V, Be), performed using thermodynamic modeling via the Thermo-Calc software package. Phase formation was investigated and compared in a commercial alloy (Al98–Fe1–Si1) and an intermetallic alloy (Al60–Fe33–Si7) under both individual and synergistic alloying conditions. The thermal characteristics (liquidus, solidus, and α- and β-transformations) and phase constituents were analyzed across a broad temperature range (0–1200 °C). It was found that the alloying elements exert diverse effects on phase stability and alloy structure, with intermetallic systems exhibiting greater thermal stability. Particular attention was given to the formation of the matrix phase and the influence of synergistic alloying on phase equilibria and the potential emergence of new stable compounds. The results provide a basis for targeted alloy design, including the use of secondary aluminum, to develop materials with tailored properties for transportation and mechanical engineering applications.</p>
	<p>Keywords: Al–Fe–Si, ThermoCalc software, intermetallic phases, phase equilibrium, synergistic alloying.</p>
<p>Andreyachshenko Violetta Alexandrovna</p>	<p>Information about author: <i>PhD, associate professor, Head of the Testing Laboratory Engineering Profile Comprehensive Development of Mineral Resources, Abylkas Saginov Karaganda Technical University, N. Nazarbayev Ave., 56, Karaganda, Kazakhstan. E-mail: v.andreyachshenko@ktu.edu.kz; ORCID ID: https://orcid.org/0000-0001-6933-8163</i></p>

Introduction

The modern development of the metal products industry requires the creation of new materials with enhanced performance characteristics, cost-effective production, and compatibility with advanced manufacturing technologies. In the context of increasing demand for lightweight, durable, and wear-resistant materials—particularly in the aerospace and automotive sectors—aluminum alloys remain among the most promising candidates due to their low density, excellent corrosion resistance, high electrical conductivity, and adequate mechanical properties [[1], [2], [3], [4], [5]].

Significant improvements in mechanical and operational properties are often achieved through additional processing techniques aimed at critical grain refinement [[6], [7], [8], [9], [10]]. However, to meet the desired performance levels, costly alloying additions—primarily rare-earth elements—are still commonly used, which significantly increases the overall production cost [[11], [12], [13], [14], [15]].

In this regard, the exploration of alternative alloying strategies aimed at improving the performance of aluminum alloys without relying on scarce and expensive elements is of particular relevance. A promising approach involves studying the ternary Al–Fe–Si system, incorporating alloying elements frequently present as impurities in aluminum alloys, which could potentially be used for the targeted modification of phase composition [[16], [17], [18], [19], [20]].

Special attention is drawn to the potential formation of the intermetallic $\text{Al}_8\text{Fe}_2\text{Si}$ phase, which possesses a highly symmetric crystal structure. This opens new pathways for developing intermetallic aluminum-based composite materials with a unique combination of strength and ductility [[21], [22], [23], [24], [25]].

Despite growing global scientific interest in Al–Fe–Si alloys [[26], [27], [28], [29], [30]], data on the influence of impurity and secondary alloying elements on their structure and properties remain limited. Particularly important is the comparative investigation of phase formation in conventionally

alloyed commercial aluminum grades and intermetallic-based materials.

This study provides a detailed investigation into phase formation mechanisms under various alloying conditions and analyzes the features of phase evolution depending on composition and thermal treatment regimes.

Accordingly, the present research is aimed at establishing a scientific basis for the alloying of aluminum intermetallic composites, enabling the design of materials with tailored properties without the use of costly alloying components. The results obtained are of interest for the development of high-reliability products intended for operation under harsh conditions and may serve as a foundation for designing new structural materials for transport and mechanical engineering applications.

Objective of the study: To compare phase formation and identify its key features in a commercial aluminum alloy and an intermetallic Al–Fe–Si alloy through thermodynamic modeling of the phase composition, using the most commonly encountered alloying elements in aluminum systems.

Experimental part

Thermodynamic modeling was carried out using the Thermo-Calc software package (version 2024a) with the TCS Al-based Alloys (TCAL8.2) database. Main modeling stages:

1. Definition of alloy compositions. At this stage, two types of alloys were studied: the commercial alloy $\text{Al}_{98}\text{Fe}_1\text{Si}_1$, alloyed both stepwise and synergistically with 10 impurity elements (Mg, Cu, Ni, Mn, Cr, Zn, Ti, Zr, V, Be, Sc). The concentrations of alloying elements varied from 0.003 to 5.4 wt.%, introduced at the expense of aluminum content. In the case of synergistic alloying, the aluminum concentration was 81.77 wt.%. For comparison, alloying of the intermetallic alloy $\text{Al}_{60}\text{Fe}_{33}\text{Si}_7$ with the same elements as in the commercial alloy was also studied. As a result of synergistic alloying, the aluminum concentration decreased to 43.77 wt.% (Table 1).

2. System creation in Thermo-Calc. The modeling process was implemented using the Graphical Mode (TCG) module. A system project was created for the multiphase Al–Fe–Si–X system, where the alloying elements and their mass fractions were added. For individual alloying, one alloying element was added to the base system at a time; for synergistic alloying, all elements were added simultaneously. For comparison, diagrams for

the base system without additives were also constructed.

Table 1 - Alloying conditions

Individual alloying, wt%	Synergistic alloying, wt%
Cu4.2	Cu4.2 Mg4.2 Mn0.9 Cr0.21 Zn5.4 Ni0.84 Ti0.12 V0.09 Zr0.27 Be0.003
Mg4.2	
Mn0.9	
Cr0.21	
Zn5.4	
Ni0.84	
Ti0.12	
V0.09	
Zr0.27	
Be0.003	

3. Setting modeling parameters. All calculations were performed under the following conditions:

- Calculation type: Equilibrium Calculation;
- Temperature range: from 1200 °C to 0 °C;
- Temperature step: 50 °C;
- Pressure: 1 atm (standard).

4. Calculation and construction of polythermal sections. After running Thermo-Calc, the equilibrium phase composition at each temperature step was calculated. Polythermal sections were built using the Plot Renderer module. The X-axis represents the volume fraction of the phase, and the Y-axis represents temperature (°C). The graph displays curves of the forming phases with a legend.

5. Interpretation of the obtained diagrams. Phases were identified, and phase transformation temperatures were evaluated. At temperatures above the liquidus, the system is completely liquid. Cooling leads to the sequential precipitation of phases: for the commercial alloy, FCC_A1 is the first to form, followed by θ and others; for the intermetallic alloy, the primary phase is θ or $\text{Al}_7\text{Cu}_4\text{Ni}$, followed by AlFeSi , Laves, and others.

The final phase composition at room temperature determines the performance properties.

6. Hardness testing of the alloyed intermetallic alloys was carried out using a Wilson VH1150 Vickers hardness tester. The chemical composition of the investigated alloys was determined using an Olympus Vanta Element S X-ray fluorescence (XRF) analyzer.

Results and Discussion

The obtained results on the influence of alloying/impurity elements on the phase composition and, consequently, on the resulting

properties indicate that the characteristics of phase transformations are highly sensitive to the aluminum content in the alloy.

When transitioning to an intermetallic state, the activity of individual elements and the thermodynamic conditions for phase formation change. Not all elements present in industrial alloys are capable of dissolving in the base phase constituents. The introduced elements form compounds with one (or several) of the base alloy components, thereby shifting the phase equilibrium and promoting the binding or, conversely, the precipitation of other elements.

The effect of individual alloying on the phase transformation temperatures of aluminum alloys is presented in Table 2, which shows the calculated temperatures of the liquidus (T_L), solidus (T_S), and the start (T_{st}) and end (T_{end}) of α - and β -phase transformations for both commercial (com) aluminum alloys and intermetallic (int) systems modified by the addition of various alloying elements (Cu, Mg, Mn, Cr, Ni, Zn, Ti, V, Zr, Be). The temperatures are given in degrees Celsius ($^{\circ}\text{C}$).

Analysis of the data makes it possible to trace both the general effect of alloying on the thermodynamic behavior of the system and the specific influence of individual elements.

In commercial alloys (T_L^{com}), a predominant decrease in the liquidus temperature is observed compared to the base alloy without alloying (650°C). The most significant reductions are noted with the addition of Mg (630°C), Zn (641°C), and Mn (630°C), indicating their strong ability to lower the melting onset temperature. Conversely, Be increases T_L^{com} to 740°C —the highest value among all elements—which may be attributed to the formation of high-melting-point compounds between Be and aluminum.

T_S^{com} also decreases with the addition of most elements. The most pronounced decrease in solidus temperature is observed with Mg (546°C) and Zn (596°C), indicating a widening of the solidification interval and a potential deterioration in casting properties. Higher T_S^{com} values are found with Cr (626°C) and Ni (615°C).

For intermetallic alloys (T_L^{int}), the liquidus temperature remains virtually unchanged (1070°C) with most alloying elements, except for Zn, where it increases to 1100°C , suggesting the formation of stable intermetallic compounds with higher melting points. In intermetallic systems (T_L^{int}), the range of values is broader – from 399°C with Zn to 680°C with Cr. Thus, intermetallic systems alloyed with Cr exhibit the most thermally stable solid state, while Zn drastically reduces the end temperature of

solidification, which may indicate the presence of low-temperature eutectics.

Given the particular interest in the α -phase in the intermetallic alloy, the effect of alloying on its formation and transformation into the low-temperature β -phase was also analyzed.

The onset temperature of α -phase formation in commercial alloys ($T_{st}^{com}\alpha$) varies within the range of 600 – 629°C . A significant reduction is observed with Mg (600°C), reflecting its impact on lowering the thermal stability of the α -phase. The addition of Mn, Cr, and Ni suppresses α -phase formation in this temperature region. $T_{st}^{int}\alpha$ in intermetallic alloys demonstrates higher values – from 650°C (Zn) to 769°C (baseline and some alloying compositions). This indicates the thermal stability of the α -phase in the intermetallic matrix and the weak influence of most alloying elements, except Zn and Mg, which noticeably lower the α -transformation onset temperature.

The α -phase transformation end temperature ($T_{end}^{com}\alpha$) ranges from 572°C (with Mg) to 629°C (without alloying), indicating a narrowing of the α -phase stability interval with alloying. Meanwhile, in intermetallic alloys, the lower boundary of α -phase stability remains almost unchanged for all additions – around 446 – 450°C , except for Zn (462°C). This may suggest the thermodynamic stability of the α -phase in intermetallic systems regardless of composition.

The onset temperature of β -phase transformation in commercial alloys ($T_{st}^{com}\beta$) shows a broader variation – from 550°C (Ni) to 612°C (unalloyed), reflecting the differing thermodynamic activity of alloying elements, with Ni significantly reducing β -phase stability. $T_{st}^{int}\beta$ remains nearly identical across all systems, at 446 – 462°C , indicating low sensitivity of this phase to the type of alloying in intermetallic compositions.

Thus, individual alloying reveals that the addition of alloying elements exerts diverse effects on phase transformation temperatures. Mg and Zn exhibit the strongest lowering effect on liquidus and solidus temperatures, while Be and Cr contribute to their increase. Intermetallic systems overall demonstrate greater phase stability compared to commercial alloys, particularly with respect to the α - and β -phases. Zn emerges as the most sensitive element affecting the thermal characteristics of both the liquidus/solidus and the phase transformations, especially in intermetallic compounds. Certain elements (e.g., Ni and Mg) can significantly narrow the phase stability temperature intervals, which must be taken into account in the

design of heat-resistant and castable aluminum alloys.

Multicomponent system modeling was subsequently performed to assess the mutual influence of the considered elements. Although the simultaneous presence of all alloying elements in an alloy is unlikely, the investigation of such a system is crucial for a deeper understanding of the synergistic alloying effect, particularly in identifying the potential formation of new phases resulting from interactions among impurity/alloying elements within an aluminum or intermetallic matrix.

At the same time, similar individual alloying effects in commercial and intermetallic alloys result in different base phases under synergistic alloying conditions. In the commercial alloy, the matrix is primarily a solid solution of aluminum, whereas in the intermetallic alloy, the θ -phase serves as the main matrix.

Analysis of polythermal sections enables conclusions to be drawn about the nature of phase transformations, crystallization features, phase composition and stability from the liquid state down to 0 °C, as well as predictions of the service properties of the resulting materials.

Figure 1 presents the polythermal sections for two alloys with different base element compositions: the commercial alloy $\text{Al}_{98}\text{--Fe}_1\text{--Si}_1$ and the intermetallic alloy $\text{Al}_{60}\text{--Fe}_{33}\text{--Si}_7$, each synergistically alloyed with ten of the most common impurity elements. The X-axis shows the volume fraction of all phases, while the Y-axis represents temperature (°C). Each colored curve corresponds to the phase fraction of one of the stable or metastable phases in the system, depending on the temperature. This allows for tracing the sequence of phase transformations upon cooling and quantifying the phase distribution.

The polythermal sections demonstrate fundamental differences in phase formation mechanisms depending on the chemical composition: from matrix α -Al systems to structures saturated with intermetallic phases.

For the $\text{Al}_{98\text{--}n_1}\text{--Fe}_1\text{--Si}_1\text{--}nX_i$ alloy, the initial melting point (liquidus) is ~ 660 °C—above which only the liquid phase exists. Upon temperature reduction, the first phase to crystallize is FCC_A1, a solid solution of alloying elements in aluminum with an FCC lattice. The volume fraction of solid aluminum remains in the range of $\approx 70\text{--}80\%$ upon further cooling down to room temperature. Thus, the aluminum matrix is retained as the primary phase, while intermetallics play a secondary role.

Below ~ 600 °C, a wide range of secondary phases emerges. The alloy exhibits the presence of

$\text{Al}_{13}\text{Fe}_4$ (θ), $\text{Al}_{15}\text{Si}_2\text{M}_4$ (where $\text{M} = \text{Mn, Cr, Ti}$), $\text{Al}_5\text{Fe}_2\text{Si}_2$, and $\text{Al}_{18}\text{Mg}_3\text{Ti}_2$, primarily forming below 600 °C. Additionally, phases such as $\text{Al}_7\text{Cu}_4\text{Ni}$, $\text{Al}_2\text{Cu_C16}$, ALZr_D023 , FEB_B27 (ZrSi), T_PHASE ($\text{Al}_2\text{Mg}_3\text{Zn}_3$), S_PHASE (Al_2CuMg), and Laves phases (C14_LAVES) are detected, indicating complex alloying, enrichment of the structure with various intermetallic inclusions, and complex multiphase eutectic crystallization. These phases form in small volume fractions and within narrow temperature intervals.

Of particular note is the formation of a cubic αC phase involving manganese and chromium atoms—an effect not observed in alloys individually alloyed with Mn or Cr. Overall, the phase structure indicates heterogeneity, but the high volume fraction of ductile aluminum matrix is preserved. This ensures good workability and impact toughness, although local strengthening and embrittlement may occur in areas with concentrated intermetallics.

For the $\text{Al}_{60\text{--}n_1}\text{--Fe}_{33}\text{--Si}_7\text{--}nX_i$ alloy, an intermetallic composition is considered, characterized by a significantly lower aluminum content (60 wt.%) and elevated Fe and Si content. The liquidus temperature of the intermetallic alloy is substantially higher, reaching ~ 1100 °C, corresponding to the presence of a large fraction of high-melting phases.

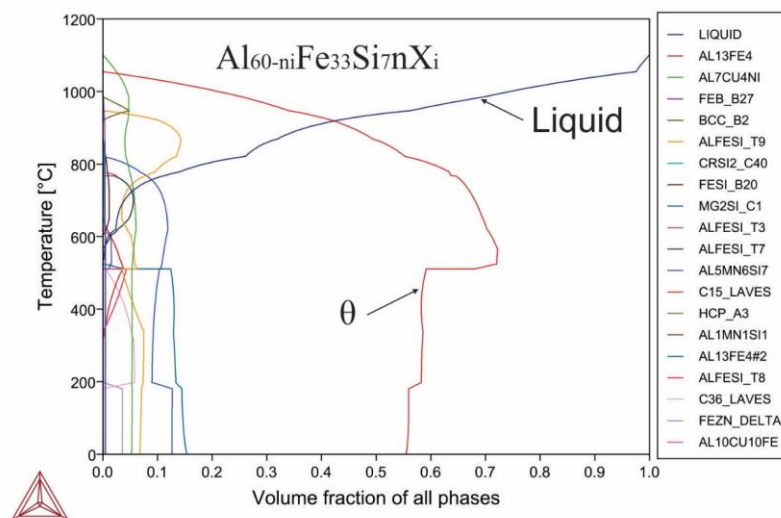
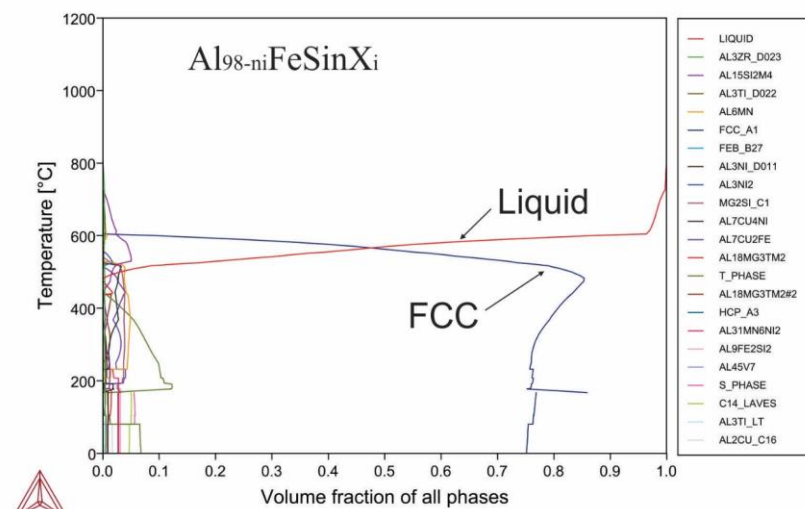
The first crystallizing phase is $\text{Al}_{13}\text{Fe}_4$ (a binary intermetallic compound), which constitutes a major part of the solid phase between 1000 and 700 °C. In contrast to the commercial alloy, the FCC phase is virtually absent, indicating replacement of the aluminum matrix with rigid intermetallic formations.

At $\sim 400\text{--}800$ °C, the dominant phases are $\text{Al}_7\text{Cu}_4\text{Ni}$, FeSi_B20 , BCC_B2 , the θ -phase, and a family of AlFeSi_T phases ($\tau_3, \tau_7, \tau_8, \tau_9$). These phases result from Fe–Si interactions within the aluminum matrix and play a key role in forming the intermetallic framework. The presence of FeSi_B20 further confirms the Fe-rich nature of the structure. The θ -phase occupies up to 70% of the volume in the 400–700 °C range, indicating high material hardness and brittleness.

Below 400 °C, numerous minor-volume phases appear, including Laves phases (C14, C15, C36), $\text{Al}_{13}\text{Fe}_{4\#2}$, $\text{Al}_5\text{Mn}_6\text{Si}_7$, and other complex structures. Of note is the presence of rigid Laves-type intermetallics, pointing to stabilizing elements within the structure. The $\text{Al}_{13}\text{Fe}_{4\#2}$ phase differs from the θ -phase by a higher content of dissolved elements, including silicon, and partial substitution of Fe atoms.

Table 2 – Effect of alloying on phase transformation temperatures

Alloying element	Indicator									
	T_L^{com}	T_L^{int}	T_S^{com}	T_S^{int}	$T_{st}^{com} \alpha$	$T_{st}^{int} \alpha$	$T_{end}^{com} \alpha$	$T_{end}^{int} \alpha$	$T_{st}^{com} \beta$	$T_{st}^{int} \beta$
-	650	1070	612	629	629	769	586	446	612	446
Cu	640	1070	546	665	600	665	572	447	572	447
Mg	630	1060	585	600	-	720	-	446	-	446
Mn	649	1070	626	680	-	762	-	450	-	462
Cr	695	1070	615	629	-	769	-	446	550	446
Ni	649	1070	606	641	621	753	606	446	606	446
Zn	641	1100	596	399	616	650	597	462	598	462
Ti	667	1070	612	630	629	767	585	446	611	446
V	652	1070	612	629	629	767	585	446	611	446
Zr	740	1070	615	629	629	769	578	446	603	446
Be	652	1070	611	620	629	768	586	446	611	446

**Figure 1** - Polythermal cutting of aluminum alloys with synergistic alloying

This system is dominated by intermetallic compounds across the entire temperature range, with almost complete absence of α -Al (FCC) and a wide stability range of the θ -phase. This indicates high stiffness and thermal stability but low plasticity. Such a structure is suitable for heat-resistant and wear-resistant materials but not for wrought (deformable) alloys.

When all investigated alloying elements are simultaneously introduced into the intermetallic alloy, the aluminum concentration decreases to 43.77 at.%, which is significantly lower than that in the commercial alloy (81.77 at.%). This reduction in the aluminum base has a critical impact on the phase composition: in none of the systems is the formation of the α -phase observed.

Moreover, in the intermetallic alloy, even the cubic α -modifications stabilized by Cr and Mn additions are absent. No formation of the low-temperature β -phase is observed either. In the commercial alloy, the β -phase originates from the cubic α -phase as a product of phase transformation, but the transition temperature is anomalously low—around 200 °C—confirming its metastable nature. The total volume fraction of all secondary phases is approximately 25%.

Upon the addition of magnesium under complex alloying conditions, the formation of Laves-type intermetallic phases is observed. In the commercial alloy, the hexagonal phase MgZn_2 appears. In the intermetallic system, two different modifications are formed: cubic MgCu_2 and hexagonal MgNi_2 , indicating magnesium's active participation in the formation of highly stable structures.

Despite the overall reduction in aluminum content, no significant increase in mutual interaction between the alloying elements is observed in the intermetallic alloy. In the commercial variant, nearly all compounds form with aluminum, with the exception of Laves phases. In contrast, the intermetallic alloy shows a tendency toward the formation of intermetallics between the alloying elements and iron.

In the commercial alloy, the synergistic effect is particularly evident in the formation of ternary intermetallic compounds involving impurity atoms. Notable phases include $\text{Al}_2\text{Mg}_3\text{Zn}_3$, Al_2CuMg , and $\text{Al}_{18}\text{Mg}_3(\text{Cr, Mn, Ti})_2$, reflecting complex interactions between the base and alloying components.

Under conditions of limited aluminum availability in the intermetallic system, new phases form, such as $\text{Al}_7\text{Cu}_4\text{Ni}$, along with compounds based on the Al–Fe–Si system. This indicates a shift in chemical equilibrium toward more complex

intermetallic compounds involving copper, iron, and nickel.

It is important to emphasize the high chemical reactivity of Cu, Mg, and Ni, which promotes the formation of stable binary and ternary phases. However, it is the available aluminum content that ultimately determines the final phase composition and the direction of interactions. The total fraction of all phases, excluding the main matrix composed of θ and θ' -modifications, reaches 30%.

In the intermetallic alloy, the earliest crystallizing phase is $\text{Al}_7\text{Cu}_4\text{Ni}$, followed by the formation of the θ -phase upon undercooling by approximately 40 °C. In the temperature range of 500–600 °C, the θ -phase content exceeds 70%. At around 510 °C, coexistence of the θ -phase with impurities in the structure is observed, indicating the formation of its substitutional modifications. As a result, at room temperature, the material consists predominantly ($\approx 70\%$) of the θ -phase with a variable elemental composition. The solidus temperature is 485 °C for the commercial alloy and 533 °C for the intermetallic alloy.

Interestingly, many elements that typically tend to form silicides lose the ability to independently form such phases under complex alloying conditions and remain in dissolved form. Exceptions include: Cr-silicide (observed only in the intermetallic system), as well as silicides of Mg and Zr. Beryllium appears as a separate phase, along with copper intermetallics and a Fe–Zn compound.

Key differences between the commercial and intermetallic alloys based on analysis of polythermal sections:

The commercial alloy retains the FCC_A1-type aluminum matrix, ensuring high ductility and good processability. Intermetallic phases are secondary and do not dominate the overall structure.

In the intermetallic alloy, α -Al is absent, and the matrix is formed by $\text{Al}_{13}\text{Fe}_4$ and AlFeSi (τ) intermetallics, which crystallize directly from the melt. This imparts increased hardness and heat resistance, but reduces formability.

The commercial alloy exhibits a more complex phase structure with numerous local phases, including compounds of Cu, V, Zr, and other elements, while the intermetallic alloy's structure is simplified, focused on forming a highly stable framework.

The onset temperature of crystallization for the intermetallic alloy (~ 850 °C) is significantly higher

than that of the commercial alloy ($\sim 650^\circ\text{C}$), indicating direct formation of the intermetallic θ -phase from the melt.

The presence of Laves phases in the intermetallic system enhances resistance to thermal and chemical exposure, but also increases brittleness.

The practical significance of the obtained results lies in their potential to predict the performance characteristics of real-world alloys. Moreover, the findings of this study may serve as a fundamental basis for selecting alloying strategies in the design of new aluminum-based alloys, including intermetallic systems, particularly in the context of synergistic alloying.

The temperature-dependent phase formation behavior under the influence of alloying elements enables control over the thermal stability of alloy properties and facilitates the development of optimized heat treatment regimes aimed at achieving target microstructures and performance characteristics.

To validate the obtained results, hardness tests were conducted on both commercial and alloyed intermetallic aluminum systems. For instance, in the intermetallic alloy with the nominal composition $\text{AlFe}_{33.59}\text{Si}_{5.18}\text{Mn}_{1.574}\text{Ni}_{0.19}$ (wt.%), the microhardness of the intermetallic phases reached 756 HV1. In contrast, the alloy with the composition $\text{AlFe}_{29.5}\text{Si}_{3.72}\text{Mn}_{0.18}\text{Ni}_{0.02}\text{Cu}_{0.02}$ (wt.%) exhibited a significantly lower microhardness of 450 HV1 for its intermetallic phases.

This difference in microhardness is primarily attributed to the presence of manganese, which promotes the coagulation of intermetallic phases and is capable of dissolving into the binary intermetallic θ -phase through partial substitution of iron atoms, thereby stabilizing the θ_2 -phase.

Meanwhile, in the commercial alloy, the microstructure is dominated by a FCC aluminum solid solution with a typical microhardness in the range of 130–135 HV1.

Conclusions

Using thermodynamic modeling methods, phase diagrams were obtained for aluminum alloys containing 1 wt.% Fe and 1 wt.% Si, as well as for the intermetallic Al–Fe–Si system alloyed with 10 industrially significant elements. The influence trends of each alloying addition on thermal characteristics and phase formation mechanisms were established.

It was found that increasing the volume fraction of the α -phase is not achievable through the addition of any of the investigated elements, regardless of their nature or concentration. The primary effect of alloying additions is manifested through the shift of phase transformation temperatures and the formation of alternative stable phases.

It was demonstrated that copper, nickel, and magnesium tend to form stable binary and ternary compounds. Their combined addition leads to the formation of Laves-type phases. In the intermetallic alloy, an increase in the amount of θ -phase was observed in each case, including modifications of its stoichiometry due to partial dissolution of impurities.

The obtained data enable targeted alloying strategies aimed at optimizing alloy properties, including the use of secondary (recycled) aluminum. These results hold practical value for the development of new composite materials and for interpreting the microstructure of industrial aluminum alloys.

Conflict of interest. On behalf of all authors, the corresponding author declares that there is no conflict of interest.

Acknowledgements. This research is funded by the Science Committee of the Ministry of Science and Higher Education of the Republic of Kazakhstan. Grant No. AP19675471 “Development of technology for the synthesis of composite ceramic materials of the AlxFeySi system using the additive method”

Cite this article as: Andreyachshenko VA. Effect of Complex Alloying on the Phase Composition and Thermal Characteristics of Al–Fe–Si Aluminum Alloys. Kompleksnoe Ispolzovanie Mineralnogo Syra = Complex Use of Mineral Resources. 2027; 340(1):117-126. <https://doi.org/10.31643/2027/6445.12>

Al-Fe-Si жүйесінің алюминий қорытпаларының фазалық құрамы мен температуралық сипаттамаларына кешенді легирлеудің әсері

Андреященко В.А.

Әбілқас Сағынов атындағы Қарағанды техникалық университеті, Қарағанды, Қазақстан

<p>Мақала келді: 8 қыркүйек 2025 Сараптамадан өтті: 26 қыркүйек 2025 Қабылданды: 3 қазан 2025</p>	<p>ТҮЙІНДЕМЕ Жұмыста Thermo-Calc бағдарламалық пакетін қолдану арқылы термодинамикалық модельдеу арқылы жүзеге асырылатын, он өнеркәсіптік маңызы бар легирлеуші элементтердің (Mg, Cu, Ni, Mn, Cr, Zn, Ti, Zr, V, Be) қосылған Al-Fe-Si жүйесінің алюминий қорытпаларындағы фазалардың түзілуінің жан-жақты талдауы берілген. Жеке және синергиялық легирленген коммерциялық қорытпадағы (Al98-Fe1-Si1) және интерметалдық қорытпадағы (Al60-Fe33-Si7) фазаның түзілуі зерттеліп, салыстырылады. Қорытпалардың температуралық сипаттамаларын (сұйықтық, солидус, α- және β-түрлендірулер) және фазалық құрамдастарды салыстыру кең температуралық диапазонда (0–1200°C) жүргізіледі. Легирлеуші элементтер қорытпалардың фазалық тұрақтылығына және құрылымына көп бағытты әсер ететіні анықталды, интерметалдық жүйелер жоғары термиялық тұрақтылықты көрсетеді. Негізгі фазаның түзілуіне, сонымен қатар синергетикалық легирлеудің фазалық тепе-теңдікке әсері мен жаңа тұрақты қосылыстардың түзілу мүмкіндігіне ерекше көңіл бөлінеді. Алынған нәтижелер көліктік және машина жасау үшін белгіленген қасиеттері бар материалдарды жасау үшін қайталама алюминийді қолдануды қоса алғанда, алюминий қорытпаларының легирленуін мақсатты бақылауға мүмкіндік береді.</p>
	<p>Түйін сөздер: Al-Fe-Si, ThermoCalc бағдарламалық қамтамасыз ету, интерметалдық фазалар, фазалық тепе-теңдік, синергиялық легирлеу.</p>
<p>Андреященко Виолетта Александровна</p>	<p>Автор туралы ақпарат: PhD, қауымдастырылған профессор, Минералдық шикізат қазбаларды кешенді игеру инженерлік бейіндегі сынақ зертханасының басшысы, Әбілқас Сағынов атындағы Қарағанды техникалық университеті, Н. Назарбаев даңғылы, 56, Қарағанды, Қазақстан. Email: v.andreyachshenko@ktu.edu.kz; ORCID ID: https://orcid.org/0000-0001-6933-8163</p>

Влияние комплексного легирования на фазовый состав и температурные характеристики алюминиевых сплавов системы Al-Fe-Si

Андреященко В.А.

Карагандинский технический университет имени Абылкаса Сагинова, Караганда, Казахстан

<p>Поступила: 8 сентября 2025 Рецензирование: 26 сентября 2025 Принята в печать: 3 октября 2025</p>	<p>АННОТАЦИЯ В работе представлен комплексный анализ фазообразования в алюминиевых сплавах системы Al-Fe-Si с добавлением десяти промышленно значимых легирующих элементов (Mg, Cu, Ni, Mn, Cr, Zn, Ti, Zr, V, Be), проведенный методом термодинамического моделирования с использованием программного комплекса Thermo-Calc. Исследовано и сопоставлено фазообразование в коммерческом сплаве (Al98-Fe1-Si1) и в интерметаллидном сплаве (Al60-Fe33-Si7) при индивидуальном и синергетическом легировании. Проведено сравнение температурных характеристик (ликвидуса, солидуса, α- и β-превращений) и фазовых составляющих сплавов в широком температурном диапазоне (0–1200 °C). Установлено, что легирующие элементы оказывают разнонаправленное влияние на фазовую стабильность и структуру сплавов, причём интерметаллические системы демонстрируют более высокую термостабильность. Особое внимание уделено формированию фазы основы, а также влиянию синергетического легирования на фазовое равновесие и возможность образования новых устойчивых соединений. Полученные результаты позволяют целенаправленно управлять легированием алюминиевых сплавов, в том числе с использованием вторичного алюминия, для создания материалов с заданными свойствами для транспортного и машиностроительного применения.</p>
	<p>Ключевые слова: Al-Fe-Si, программное обеспечение ThermoCalc, интерметаллидные фазы, фазовое равновесие, синергетическое легирование.</p>
<p>Андреященко Виолетта Александровна</p>	<p>Информация об авторе: PhD, ассоциированный профессор, руководитель испытательной лаборатории инженерного профиля Комплексное освоение ресурсов минерального сырья, Карагандинский технический университет имени Абылкаса Сагинова, пр. Н. Назарбаева, 56, Караганда, Казахстан. Email: v.andreyachshenko@ktu.edu.kz; ORCID ID: https://orcid.org/0000-0001-6933-8163</p>

References

- [1] Padalko AG, Pyrov MS, Karelin RD, Yusupov VS, Talanova GV. Barothermal Treatment, Cold Plastic Deformation, Microstructure and Properties of Binary Silumin Al–8 at % Si. *Russ. Metall.* 2021; 1155–1164. <https://doi.org/10.1134/S0036029521090123>
- [2] Becker H, Thum A, Distl B, Kriegel MJ, Leineweber A. Effect of melt conditioning on removal of Fe from secondary Al–Si alloys containing Mg, Mn, and Cr. *Metallurgical and Materials Transactions A.* 2018; 49:6375–6389. <https://doi.org/10.1007/s11661-018-4930-7>
- [3] Arbeiter J, Vončina M, Volšak D, Medved J. Evolution of Fe-based intermetallic phases during homogenization of Al–Fe hypoeutectic alloy. *Journal of Thermal Analysis and Calorimetry.* 2020; 142(5):1693–1699. <https://doi.org/10.1007/s10973-020-10161-8>
- [4] Lee JY, Heo H, Kang N, Kang CY. Microstructural Evolution of Reaction Layer of 1.5 GPa Boron Steel Hot-Dipped in Al–7wt% Ni–6wt% Si Alloy. *Metals.* 2018; 8(12):1069. <https://doi.org/10.3390/met8121069>
- [5] Khan MH, Das A, Li Z, Kotadia HR. Effects of Fe, Mn, chemical grain refinement and cooling rate on the evolution of Fe intermetallics in a model 6082 Al-alloy. *Intermetallics.* 2021; 132:107132. <https://doi.org/10.1016/j.intermet.2021.107132>
- [6] Kocich R, Kunčická L. Optimizing Structure and Properties of Al/Cu Laminated Conductors via Severe Shear Strain. *J. Alloys Compd.* 2023; 953:170124. <https://doi.org/10.1016/j.jallcom.2023.170124>
- [7] Wang C, Yu F, Zhao D, Zhao X, Zuo L. Microstructure Evolution of Al–15% Si Alloy during Hot Rolling. *Philos. Mag. Lett.* 2018; 98:456–463. <https://doi.org/10.1080/09500839.2019.1573332>
- [8] Cepeda-Jiménez CM, García-Infanta JM, Zhilyaev AP, Ruano OA, Carreño F. Influence of the Supersaturated Silicon Solid Solution Concentration on the Effectiveness of Severe Plastic Deformation Processing in Al–7wt.% Si Casting Alloy. *Mater. Sci. Eng. A.* 2011; 528:7938–7947. <https://doi.org/10.1016/j.msea.2011.07.016>
- [9] Andreyachshenko VA. Finite element simulation (FES) of the fullering in device with movable elements. *Metalurgija.* 2016; 55(4):829–831.
- [10] Naizabekov AB, Andreyachshenko VA, Kliber J, Kocich R. Tool for realization several plastic deformation. In: 22th International Conference on Metallurgy and Materials METAL; Brno, Czech Republic. 2013, 317–321.
- [11] Belov NA, Alabin AN, Matveeva IA, Eskin DG. Effect of Zr additions and annealing temperature on electrical conductivity and hardness of hot rolled Al sheets. *Trans. Nonferrous Met. Soc. China.* 2015; 25:2817–2826. [https://doi.org/10.1016/S1003-6326\(15\)63907-3](https://doi.org/10.1016/S1003-6326(15)63907-3)
- [12] Jiang H, Li S, Zhang L, He J, Zheng Q, Song Y, et al. The influence of rare earth element lanthanum on the microstructures and properties of as-cast 8176 (Al–0.5 Fe) aluminum alloy. *Journal of Alloys and Compounds.* 2021; 859:157804. <https://doi.org/10.1016/j.jallcom.2020.157804>
- [13] Chen Y, Xiao C, Zhu S, Li Z, Yang W, Zhao F, et al. Microstructure characterization and mechanical properties of crack-free Al–Cu–Mg–Y alloy fabricated by laser powder bed fusion. *Additive Manufacturing.* 2022; 58:103006. <https://doi.org/10.1016/j.addma.2022.103006>
- [14] Zhu H, Li J. Advancements in corrosion protection for aerospace aluminum alloys through surface treatment. *International Journal of Electrochemical Science.* 2024; 19(2):100487. <https://doi.org/10.1016/j.ijoes.2024.100487>
- [15] Fan T, Ruan Z, Zhong F, Xie C, Li X, Chen D, et al. Nucleation and growth of L12–Al3RE particles in aluminum alloys: A first-principles study. *Journal of Rare Earths.* 2023; 41(7):1116–1126. <https://doi.org/10.1016/j.jre.2022.05.018>
- [16] Wang T, Chen C, Ma J, Wei S, Xiong M, et al. Influence of Si on the intermetallic compound formation in the hot-dipped aluminide medium carbon steel. *Materials Characterization.* 2023; 197:112700. <https://doi.org/10.1016/j.matchar.2023.112700>
- [17] Sersour Z, Amirouche L. Effect of Alloying Additions and High Temperature T5-Treatment on the Microstructural Behavior of Al–Si-Based Eutectic and Hypo-Eutectic Alloys. *Int. J. Met.* 2022; 16:1276–1291. <https://doi.org/10.1007/s40962-021-00676-7>
- [18] Alemdag Y, Karabiyik S, Mikhaylovskaya AV, Kishchik, M.S.; Purcek, G. Effect of Multi-Directional Hot Forging Process on the Microstructure and Mechanical Properties of Al–Si Based Alloy Containing High Amount of Zn and Cu. *Mater. Sci. Eng. A.* 2021; 803:140709. <https://doi.org/10.1016/j.msea.2020.140709>
- [19] Tsaknopoulos K, Walde C, Tsaknopoulos D, Cote DL. Evolution of Fe-Rich Phases in Thermally Processed Aluminum 6061 Powders for AM Applications. *Materials.* 2022; 15(17):5853. <https://doi.org/10.3390/ma15175853>
- [20] Zhang X, Wang D, Li X, Zhang H, Nagaumi H. Understanding crystal structure and morphology evolution of Fe, Mn, Cr-containing phases in Al–Si cast alloy. *Intermetallics.* 2021; 131:107103. <https://doi.org/10.1016/j.intermet.2021.107103>
- [21] Fang CM, Que ZP, Fan Z. Crystal chemistry and electronic structure of the β -AlFeSi phase from first-principles. *Journal of Solid State Chemistry.* 2021; 299:122199. <https://doi.org/10.1016/j.jssc.2021.122199>
- [22] Que Z, Fang C, Mendis CL, Wang Y, Fan Z. Effects of Si solution in θ -Al13Fe4 on phase transformation between Fe-containing intermetallic compounds in Al alloys. *Journal of Alloys and Compounds.* 2023; 932:167587. <https://doi.org/10.1016/j.jallcom.2022.167587>
- [23] Wang M, Guo Y, Wang H, Zhao S. Characterization of Refining the Morphology of Al–Fe–Si in A380 Aluminum Alloy Due to Ca Addition. *Processes.* 2022; 10(4):672. <https://doi.org/10.3390/pr10040672>
- [24] Xia X, Chen M, Lu Y-J, Fan F, Zhu C, Huang J, Deng T, Zhu S. Microstructure and Mechanical Properties of Isothermal Multi-Axial Forging Formed AZ61 Mg Alloy. *Trans. Nonferrous Met. Soc. China.* 2013; 23:3186–3192. [https://doi.org/10.1016/S1003-6326\(13\)62851-4](https://doi.org/10.1016/S1003-6326(13)62851-4)
- [25] Kocich R. Effects of Twist Channel Angular Pressing on Structure and Properties of Bimetallic Al/Cu Clad Composites. *Mater. Des.* 2020; 196:109255. <https://doi.org/10.1016/j.matdes.2020.109255>

- [26] Asadikiya M, Yang S, Zhang Y, Lemay C, Apelian D, Zhong Y. A Review of the Design of High-Entropy Aluminum Alloys: A Pathway for Novel Al Alloys. *J. Mater. Sci.* 2021. 56: 12093–12110. <https://doi.org/10.1007/s10853-021-06042-6>
- [27] Aranda VA, Figueroa IA, González G, García-Hinojosa JA, Alfonso I. Study of the microstructure and mechanical properties of Al-Si-Fe with additions of chromium by suction casting. *Journal of Alloys and Compounds.* 2021; 853:157155. <https://doi.org/10.1016/j.jallcom.2020.157155>
- [28] Pang N, Shi Z, Wang C, Li N, Lin Y. Influence of Cr, Mn, Co and Ni Addition on Crystallization Behavior of Al₁₃Fe₄ Phase in Al-5Fe Alloys Based on ThermoDynamic Calculations. *Materials.* 2021; 14(4):768. <https://doi.org/10.3390/ma14040768>
- [29] Hemachandra M, Mamedipaka R, Kumar A, Thapliyal S. Investigating the Microstructure and Mechanical Behavior of Optimized Eutectic Al Si Alloy Developed by Direct Energy Deposition. *J. Manuf. Process.* 2024; 110:398–411. <https://doi.org/10.1016/j.jmapro.2024.01.002>
- [30] Cheng W, Liu CY, Ge ZJ. Optimizing the Mechanical Properties of Al–Si Alloys through Friction Stir Processing and Rolling. *Mater. Sci. Eng. A.* 2021; 804:140786. <https://doi.org/10.1016/j.msea.2021.140786>